

Electronic structure of actinide antimonides and tellurides from photoelectron spectroscopyT. Durakiewicz,^{1,2} J. J. Joyce,¹ G. H. Lander,^{1,3} C. G. Olson,⁴ M. T. Butterfield,¹ E. Guzewicz,^{1,5} A. J. Arko,¹ L. Morales,¹ J. Rebizant,³ K. Mattenberger,⁶ and O. Vogt⁶¹*Los Alamos National Laboratory, Los Alamos, New Mexico 87545, USA*²*Institute of Physics, University of Maria Curie Skłodowska, Lublin 20-031, Poland*³*European Commission, JRC, Institute for Transuranium Elements, Postfach 2340, 76125 Karlsruhe, Germany*⁴*Ames Laboratory, Iowa State University, Ames, Iowa 50011, USA*⁵*Institute of Physics, Polish Academy of Sciences, 02-668 Warsaw, Poland*⁶*Laboratorium für Festkörperphysik, ETH, CH-8093 Zurich, Switzerland*

(Received 27 February 2004; published 3 November 2004)

Single crystals of USb, NpSb, PuSb, UTe, NpTe and PuTe were investigated by photoelectron spectroscopy, this included angular-resolved studies on the U compounds. The spectral features show little dependence on incident photon energy, suggesting they all contain comparable amounts of $5f$ and conduction character. In the case of USb interesting (and unexpected) momentum dependent effects are observed in the angular-resolved studies. In PuTe, we confirm the presence of a strong three-peak structure near E_F , which has been interpreted as the signature of an intermediate valence state in similar materials. Hybridization of the $5f$ electrons with the conduction band is found within the series and the level of localization is shown to increase from Te to Sb. A surprising correlation between the binding energy of the peak bearing most of the $5f$ weight in the photoemission spectrum and the magnetic moment is discovered within the series, for which some explanations are suggested.

DOI: 10.1103/PhysRevB.70.205103

PACS number(s): 79.60.-i, 71.28.+d, 74.25.Jb

I. INTRODUCTION

Actinide compounds exhibit a wide variety of complex physics due to the interplay of the various electron states; in particular the $5f$ states may be localized or itinerant, and, in addition, may hybridize to a varying degree with electron states of anions in compounds and the actinide conduction states. In this study we have investigated by a variety of photoemission techniques the actinide monoantimonides and monotellurides. These materials, with the generic formula AnSb and AnTe, (An=U, Np, and Pu), have been widely investigated in the past, particularly their magnetic properties. They form part of a larger mononictide and monochalcogenide series.^{1,2} These compounds have a simple fcc NaCl structure, which, together with a large body of experimental work, has also generated a number of theoretical studies.¹ Herein, we present the first reports of photoemission studies for both PuTe and NpTe.

A number of motivations led to this study. First, the availability of single crystals for *all* materials meant that many of the previous concerns related to surface contamination could be eliminated, especially since the photoemission technique used included the capability for laser cleaning of the surfaces which was utilized for the Np and Pu compounds. Next, recently some work has been published by Gouder *et al.*³ on thin films of PuSe and PuSb prepared *in situ*. Dramatic differences between the photoemission spectra of these two materials were observed. Our study aimed to address the questions of whether the same differences can be observed using single crystals, and if any of these effects are strongly energy dependent. Our capabilities in this study included a tuneable incident photon energy up to 110 eV, rather than being limited to the small range of the He_I and He_{II} lines of the

conventional spectrometer (<41 eV). Finally, we were able also to perform angular resolved studies of the USb and UTe single crystals at the Synchrotron Radiation Center in Madison, Wisconsin.

Our aim has been to integrate our knowledge of the magnetism of these compounds with the photoemission spectra, and attempt to establish some systematics across the actinide series, U, Np, and Pu as the $5f$ shell is progressively filled. We conclude with a somewhat startling relationship we have found between the ordered moment and the binding energy of the main peak in the photoelectron spectra.

II. EXPERIMENTAL METHODS

Single crystals of all materials were grown by the mineralization technique⁴ with the uranium crystals grown at ETH in Zürich, and the transuranium crystals grown at ITU, Karlsruhe.

The majority of experiments were performed in the laboratories of the MST-10 Group, Los Alamos National Laboratory. A VSW HA100 electron energy analyzer working in the angle-integrated mode with ± 8 degrees acceptance angle was used for energy analysis of photoemitted electrons. The original system was modified and improved by the addition of a multichannel plate detector and a phosphorescent screen, coupled optically with a CCD camera to count the electron events. The measurement system is equipped with a custom designed He discharge lamp,⁵ compatible with a radioactive work environment. The photon energies utilized when using the He lamp as an excitation source were: 21.2 eV (He_I line), 40.8 eV (He_{II α} line) and 48.4 eV (He_{II β} line). Energy resolution was 50 meV at 40.8 eV photon energy. All measurements were performed on single crystals. A KrF excimer

TABLE I. Selected physical properties, after Ref. 2 if not stated otherwise. The errors on the magnetic moments are $\sim 0.1 \mu_B$, and those on γ about 10%.

Compound	Lattice constant [Å]	Long-range ordering	Transition temperature [K]	Magnetic moment [μ_B] at $T=0$ K	Electronic specific heat, γ [mJ/mol K ²]
USb	6.191	AF, 3k- <i>I</i>	214 ^a 213	2.85	4.36–4.56 ^b
NpSb	6.254	AF, 3k- <i>I</i>	202	2.5	?
PuSb	6.240	AF, 1k inc.	85		20
		FM	70	0.74	^c
UTe	6.155	FM	104	2.25	10.3 ^b
NpTe	6.198	AF, 4k- <i>II</i>	40	1.4	130 ^d
PuTe	6.151	Paramagn.	n.a.	n.a.	30 ^d

^aReference 19.

^bReference 10.

^cReference 41.

^dReference 28.

laser of 248 nm wavelength and 20 nsec pulse length with 10 Hz repetition rate was used to laser ablate the surface in a vacuum better than 8×10^{-11} Torr prior to measurement. Cleaning was performed by rastering a beam focused to a power density of 10^8 W/cm² across the sample surface.

The LANL facility includes a Laser Plasma Light Source (LPLS)^{6,7} that allows the incident photon energy to be varied between ~ 20 and 110 eV. The significance of using a variable photon energy source is to exploit the strong changes in the intensity of the *5f* emission as a function of incident photon energy. There is a difference in the cross section for the actinide *5f* levels and conduction states between the He_I(21.2 eV) and He_{II}(40.8 eV) lines, but this difference can be further accentuated by extending the energy range with the LPLS. The energy resolution was 100 meV at 76 eV photon energy.

The final set of measurements, which, due to regulatory concerns could be performed only on the uranium samples, was made at the Synchrotron Radiation Center, Stoughton, Wisconsin, using the Plane Grating Monochromator (PGM) beamline. In the 1980's, Reihl *et al.*⁸ studied the electronic structure of cleaved single crystals of UAs_xSe_{1-x}, U_xTh_{1-x}Sb, U_xY_{1-x}Sb, and USb_xTe_{1-x} with an energy resolution of 150 meV, and an analyzer collecting 86° in the angle-integrated mode and 6° in the angle-resolved mode. In our angular resolved photoemission (ARPES) study we utilized a PGM beamline with an electron energy analyzer system capable of 25 meV energy resolution at 34 eV and a 1° acceptance angle. We also utilized the Erg-Seya line with a resolution of 40 meV for the low photon energies, whenever the high-order light background was a drawback or if the PGM was not accessible. Uranium compounds investigated by ARPES were oriented using a Laue camera and cleaved in a vacuum better than 5×10^{-11} Torr prior to measurement. The samples did not show signs of surface degradation over the duration of experiment. The sample temperatures, except for the temperature-dependent UTe study, were 12 K for USb and UTe, 15 K for NpTe and PuSb and 80 K for NpSb and PuTe.

III. RESULTS AND DISCUSSION

The *5f* compounds of the NaCl type structure constitute a group particularly suitable for determining systematics due to their very similar lattice parameters. Below we discuss the individual compounds and subsequently our findings related to the systematics within the series. Basic physical properties of the investigated compounds are given in Table I.

In Fig. 1 we show a comparison of angle-integrated spectra between each mononictide and monochalcogenide. Note that the compounds USb and UTe were not examined with the conventional He lamp photon source, but rather the angle-resolved synchrotron data, taken at a slightly lower energy, and with better resolution, have been numerically angle integrated for comparison with the angle-integrated analyzer output. This numerical integration helps facilitate the comparisons between uranium and the transuranium systems. In Fig. 2 the comparisons of all three mononictides and three monochalcogenides are shown. Details of the PES spectral features will be discussed below. In general, we find one (NpSb, PuSb), two (UTe, NpTe), three (USb) or four (PuTe) well defined *5f* character peaks within the first 3 eV of each spectrum. The full width at half maximum (FWHM) of the peaks becomes smaller with diminishing binding energy. To illustrate this we plot in Fig. 3 the observed FWHM as a function of binding energy for the observed photoemission peaks. We name the peak close to the Fermi energy (E_F) “*F*” (first), whereas the broadest peak in each spectrum is called “*B*” (broad). Peak *B* exists in each case and bears the majority of the spectral *5f* weight. By virtue of the greater binding energy of peak *B* we suggest that it represents the more localized feature in the spectrum. Spectral parameters of peaks *F* and *B* in each angle-integrated spectrum are given in Table II.

A. USb

Uranium monoantimonide, USb, is an antiferromagnet with $T_N=214$ K and a commensurate ($\mathbf{k}=1$) triple- \mathbf{k} type of magnetic ordering, with the moments aligned along $\langle 111 \rangle$.²

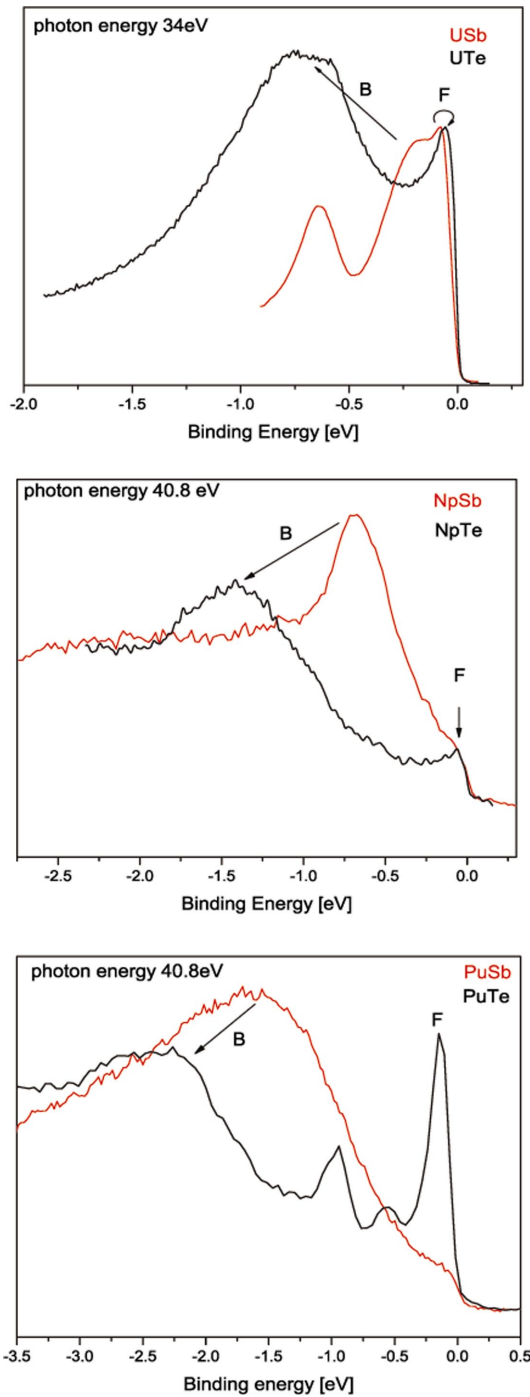


FIG. 1. (Color) Angle-integrated PES results for AnSb and AnTe series, part 1.

A localized nature for this compound was inferred from a variety of experimental results, including large magnetic moment,² the presence of well-defined excitations in the neutron inelastic scattering spectrum,⁹ and a small electronic specific heat coefficient¹⁰ (see Table I). A trivalent or nearly trivalent uranium configuration, $5f^3$ is commonly accepted.

The results of de Haas van Alphen (dHvA) experiments^{11,12} were unable to determine whether the $5f$ electrons in USb contribute to the Fermi surface volume. Based on a modified augmented spherical wave method

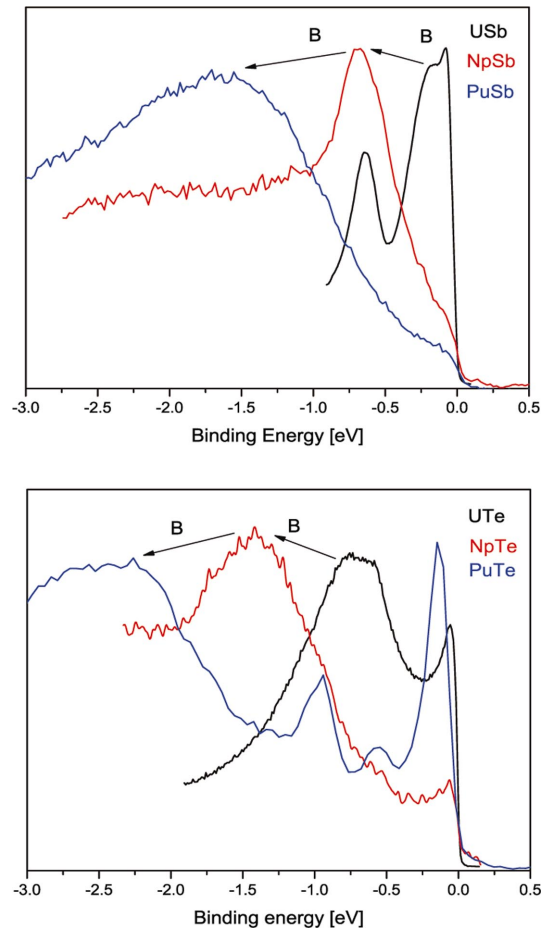


FIG. 2. (Color) Angle-integrated PES results for AnTe and AnSb series, part 2.

(MASW) it was later suggested¹³ that there are three bands crossing the Fermi level around the X symmetry point. In the first attempt at high resolution angle-resolved photoemission

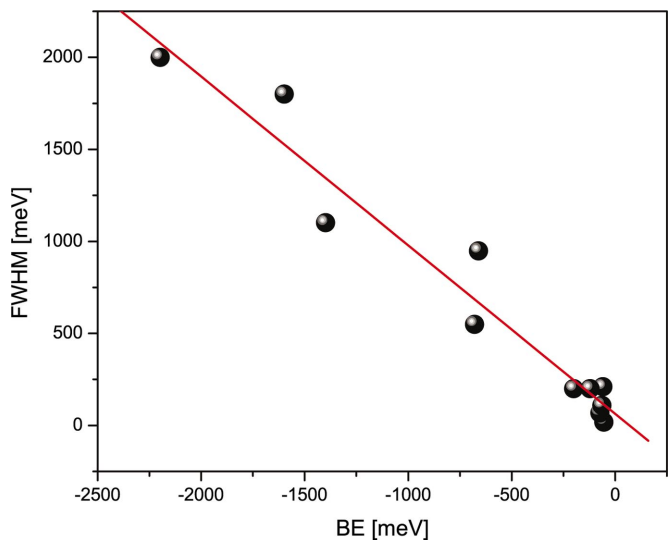


FIG. 3. (Color) FWHM versus binding energy (BE) dependence for peaks F and B. Straight line is a quadratic best fit—guide to the eye.

TABLE II. Low temperature spectral properties of peaks F and B in the angle-integrated PES spectra. Values correspond to spectra presented in Figs. 1 and 2. The values of the binding energy and full width at half maximum are obtained by numerical fitting. Errors on these values are ± 5 meV for peak *F* and ± 20 meV for peak *B*.

Compound	Peak <i>F</i>		Peak <i>B</i>		Photon energy
	BE [meV]	FWHM [meV]	BE [meV]	FWHM [meV]	
USb	-55 to -75	20 to 70	-210	200	34.0
UTe	-60	210	-660	950	34.0
NpSb	n.a.	n.a.	-680	550	40.8
NpTe	-64	110	-1400	1100	40.8
PuSb	n.a.	n.a.	-1600	1800	40.8
PuTe	-120	200	-2200	2000	40.8

by Kumigashira *et al.*¹⁴ it was found that there are *two* dispersionless bands in the Γ -*X* direction, with band *F* being closest to E_F , but not crossing it. Although the basic properties of USb seem to be well documented, the electronic structure itself is controversial with the role of *5f* electrons still difficult to establish. The concept of “dual *5f* character” is frequently utilized to describe the *5f* electrons in USb, in the sense that some of the the *5f* states look like the itinerant *3d* electrons and some are localized like the *4f* electrons.¹⁴

In Figs. 1 and 2 one may see that within the first eV below E_F there are at least three well-resolved peaks in USb, *F*, *B* and an unnamed peak, positioned at approximately 55 meV, 210 meV and 610 meV below E_F , respectively. This work was done on the PGM line at the Synchrotron Radiation Center. The experimental resolution measured at the Pt Fermi edge in our experiments was better than 25 meV. In Kumigashira’s He lamp work¹⁴ peaks *F* and *B* were not separated, due to lower energy resolution (50 meV). Furthermore, these authors state that the resolution could not be increased because of surface contamination limiting the time of experiment. This suggests that surface oxidation could have influenced the spectra presented in Ref. 14 making it more difficult to distinguish between peaks *F* and *B*. In the current ARPES study we have utilized synchrotron light instead of a He lamp and a very clean UHV environment, which allowed us to increase both the resolution and the collection time for the data sets.

In Figs. 4 and 5 we present ARPES data taken with high resolution of 25 meV on the PGM line, and with resolution of 40 meV on the Erg-Seya line. In the high resolution PGM - ARPES study presented in Fig. 4 the following points are noteworthy. (i) Peak *F* shows between 15 and 60 meV of dispersion, depending on crystallographic direction. (ii) The maximum photoemission intensity is seen away from the high symmetry points. (iii) Peak *F* represents a band that does not cross E_F . It may be noted that peak *F* is centered about 45 meV below E_F at its point of closest-approach to E_F . In Fig. 5. we present three cuts through reciprocal space in the high symmetry directions of USb, namely cuts a, b, and c, mapped on the Brillouin zone. Dispersion plots show local binding energy maxima at the *X* and *W* points, local maximum within the *W-K-W* face and a local minimum between the *X* and *W* high symmetry points.

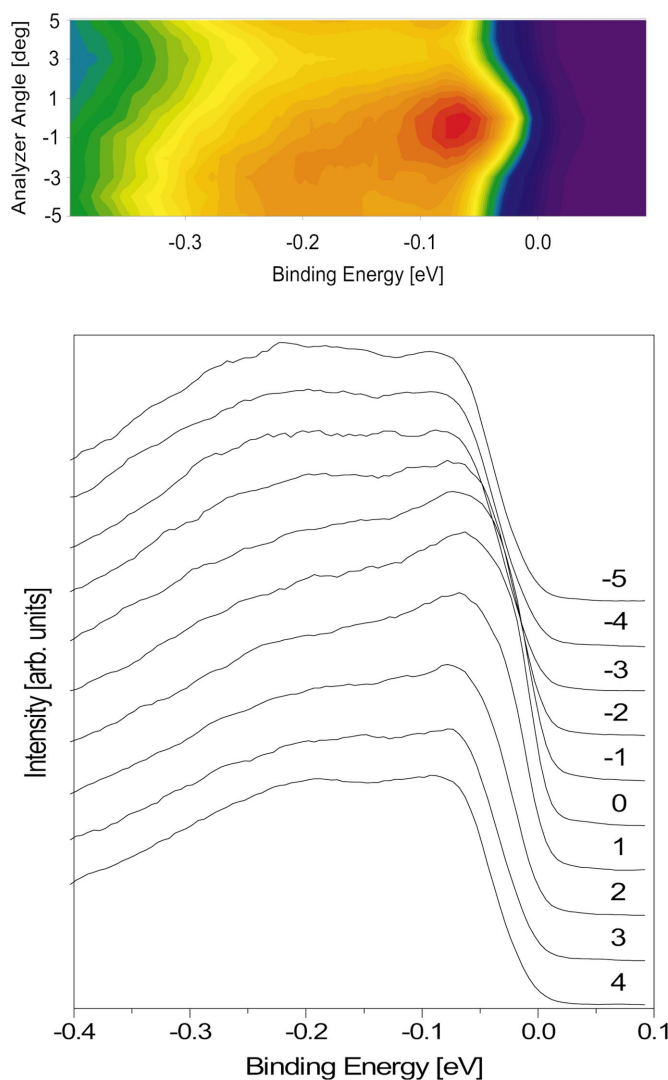


FIG. 4. (Color) USb ARPES data as a function of analyzer angle. Note significant dispersions (contrary to UTe). Peak position from the same data set is plotted also as “cut a” in Fig. 5. Color scale on the upper panel represents the photoemission signal intensity in arbitrary units, with red color indicating maximum intensity and dark blue indicating minimum intensity.

USb ARPES

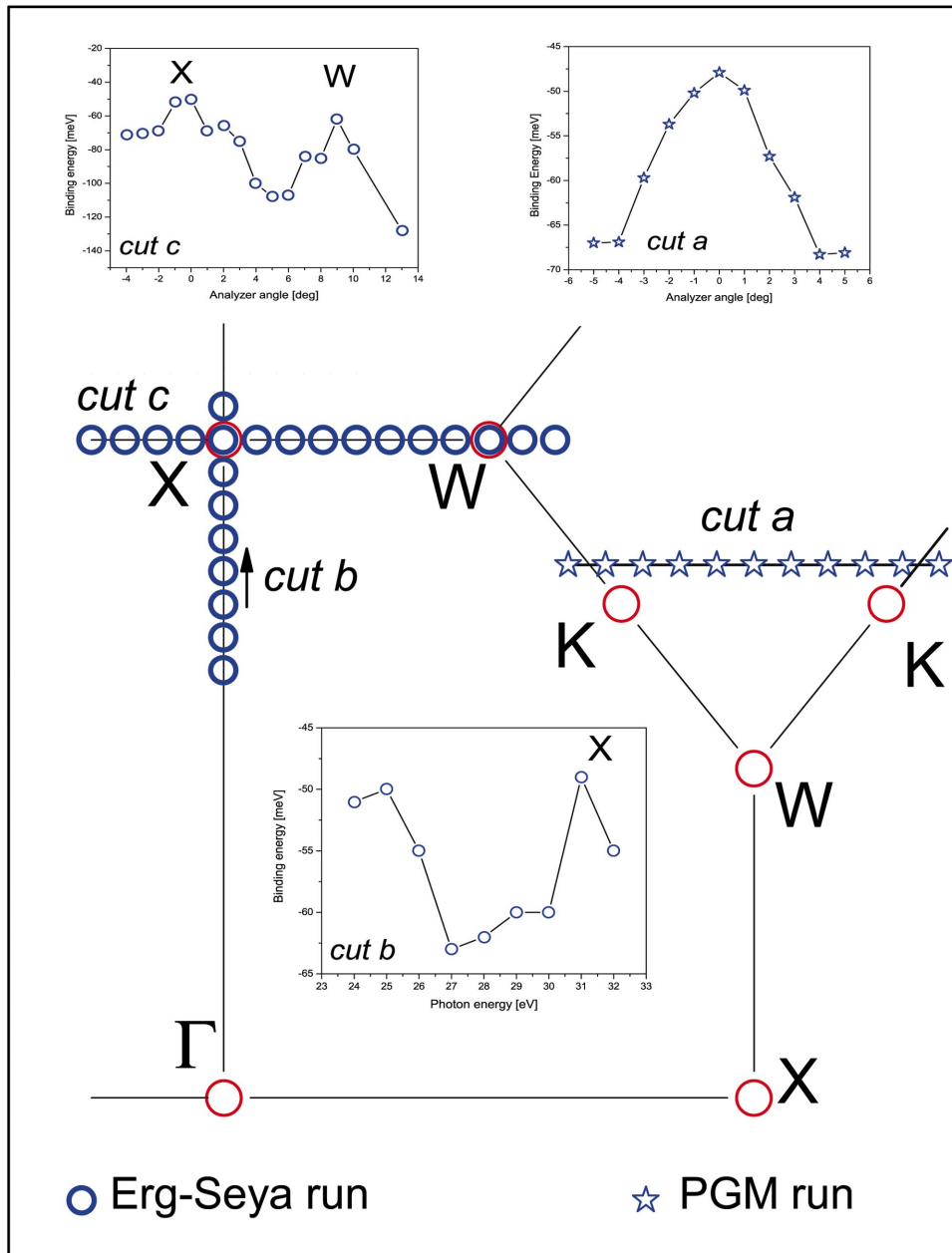


FIG. 5. (Color) USb, ARPES study of the dispersion of the first peak. Cuts “a” and “c” were obtained by varying the analyzer horizontal angle, whereas cut “a” was taken with an additional 5 degrees of vertical rotation. Cut “b” was obtained at normal emission.

The existence of a three-peak structure and the related dispersions has not previously been measured in detail for USb. Large difference between the on- and off-resonance curves shown in Fig. 6 confirms a dominating $5f$ character within the first eV of the spectrum. The location of a peak near E_F makes it difficult to employ the commonly used multiplet explanation for the USb spectrum.^{15,16} The first intermultiplet with the $5f^3:4I_{9/2}$ manifold is at 500 meV in USb. Moreover, such a multiplet transition $4I_{9/2} \rightarrow 4I_{11/2}$ should show no dispersion, i.e., be constant in k -space. Instead we find *three* peaks within this range, all of which vary in intensity with k , indicating dispersion. This is unexpected because in the calculated $5f^2$ final state one finds only one 3H_4 level within the first 500 meV from E_F , in which range

we indicate two peaks, F and B . The 3H_5 level is not seen in this work, or in previous measurements.¹⁴ Only one out of the three levels which may be associated with 3F_2 is found both here and in Ref. 14 in accordance with multiplet theory.

Neither the existence nor the dispersive character of the three $5f$ bands close to E_F was predicted by previous calculations (see Ref. 14 and references therein). Furthermore, dispersive, periodic electronic structure indicating bands is inconsistent with a localized, multiplet interpretation. Spectral analysis of band F provides additional information. In Fig. 7 we show the FWHM of peak F as a function of the binding energy. The quadratic fit is consistent with conventional behavior of a dispersive band. We therefore conclude that peaks F and B represent dispersive narrow $5f$ bands, not

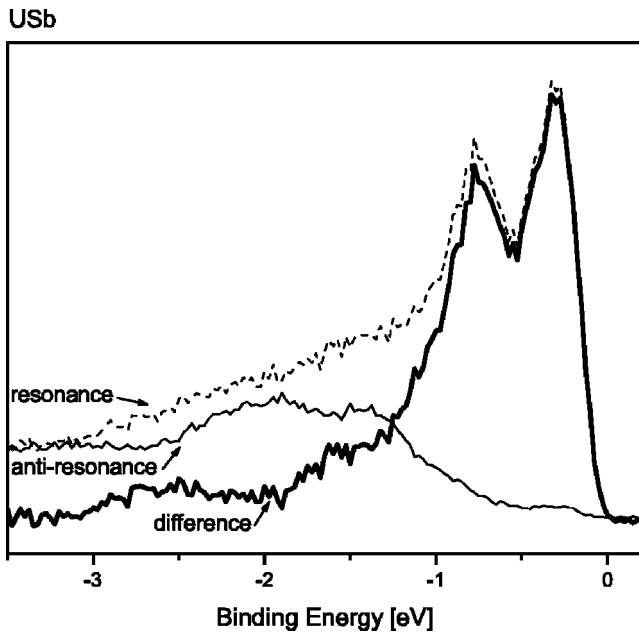


FIG. 6. Resonance study. Resonance scan was taken at photon energy 95.75 eV and anti-resonance at 91.25 eV, respectively.

crossing E_F . Detailed photon energy dependent normal emission studies will be performed in the future to determine the degree of hybridization of these bands.

B. UTe

The monochalcogenide UTe is a ferromagnet² with $T_c = 104$ K of a semi-metallic character. Fluctuating or intermediate valence was suggested as coexisting with ferromagnetism.^{17,18} As in the other compounds, the $5f$ electrons and their interaction with $6d-7s$ conduction bands plays an important role, as indicated by transport properties¹⁹ and earlier photoemission results.²⁰ From these experiments UTe

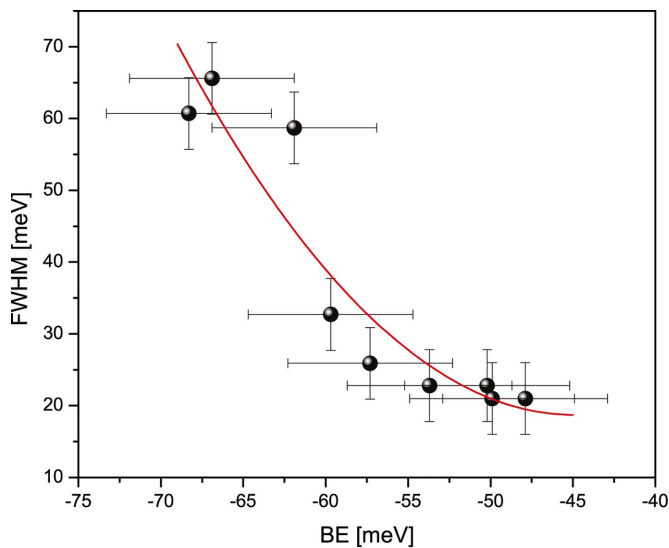


FIG. 7. (Color) USB, peak F . FWHM dependence on binding energy. Error bars ± 5 meV.

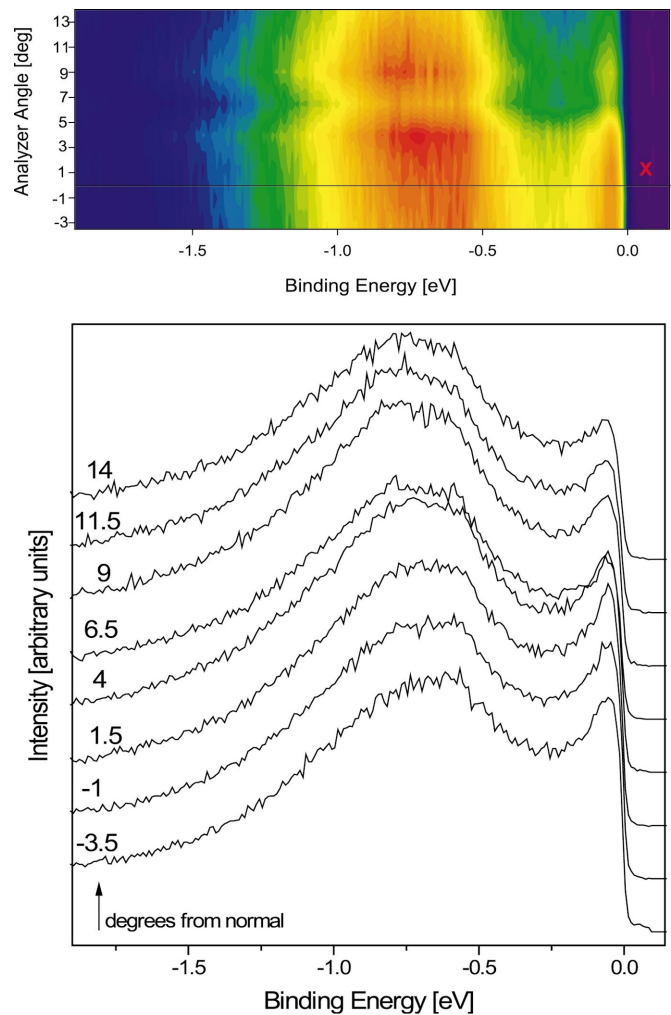


FIG. 8. (Color) UTe ARPES study at 34 eV photon energy. Line in the upper inset represents position closest to the X point along the X - Γ direction. Color scale is the same as in Fig. 4.

was interpreted as a Kondo system with a strong interaction between the $5f$ and conduction electrons. Some support for this comes from neutron inelastic scattering experiments,^{21,22} and the interpretation of these experiments in terms of anisotropic $5f$ -conduction electron interactions.²³ Strong f - p hybridization was suggested in all uranium monochalcogenides²⁴ to explain the magnetic anisotropy found within the series, which is inconsistent with the Kondo interpretation. Photoemission results^{8,20} were interpreted within the framework of a quasi-localized $5f^3$ configuration. The double-peak structure near E_F was interpreted, similar to that in USB, as a result of the $5f^2$ final-state multiplet; findings which do not seem consistent with the current PES results.

In our photoemission study we have focused on the near- E_F region examined with better energy and momentum resolution than before, obtaining an energy resolution of 25 meV and an angular resolution corresponding to 1 degree. The Γ - X ARPES results shown in Fig. 8 exhibit a structure composed of two bands, where band B might be a superposition of more than one feature. Only a minor change in intensity is seen around the X point.

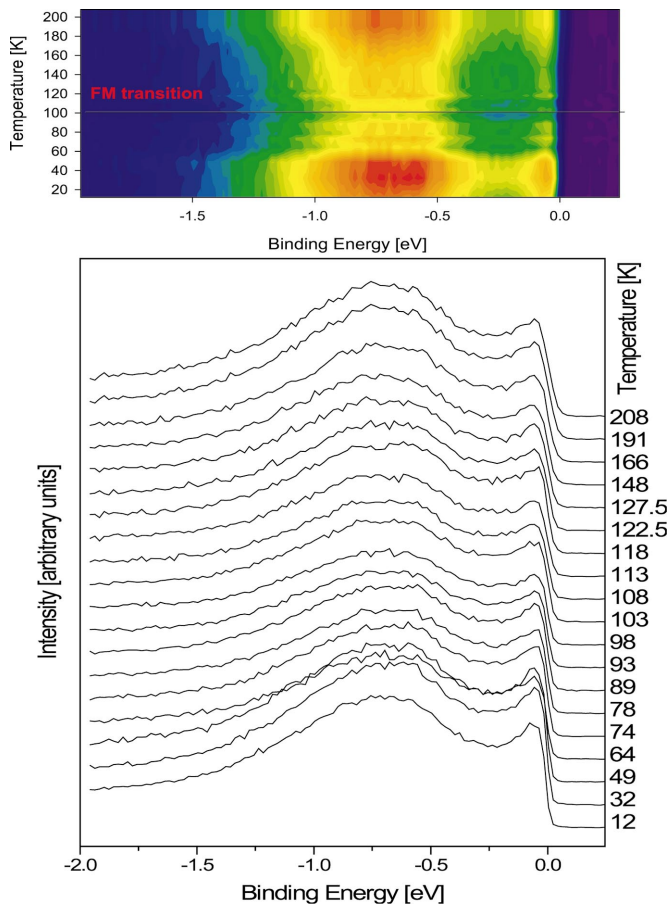


FIG. 9. (Color) UTe temperature dependent normal emission study at 34 eV photon energy. Color scale is the same as in Fig. 4.

In the past, the temperature-dependent photoemission study was employed with limited success to uranium compounds. For example, temperature dependent features in the itinerant antiferromagnet UN were observed previously with 150 meV resolution¹⁶ and interpreted as a result of folding the band states into the new antiferromagnetic (AF) Brillouin zone created by doubling the unit cell in the AF state. This finding was contrary to that previously published in Ref. 25, where no temperature dependent features were found in UPS spectra taken between 18 and 298 K. Because the temperature of the transition is relatively low in UTe (104 K compared to the 215 K in USb), it is possible to examine the change in the bands below the ordering temperature without appreciable broadening from the Fermi function. Major changes in photoemission intensity are seen around the ferromagnetic transition as shown in Fig. 9. Band F in this figure shows a distinct crossing of E_F at the transition, as shown in detail in Fig. 10. Since the FWHM of peak F is of the order of 200 meV, and its BE at low temperatures is about -55 meV, one cannot state that an actual gap is formed below the transition, as suggested in Ref. 8. Details of FWHM and BE values for both peaks F and B in UTe as a function of temperature are shown in Fig. 11. Peak B also changes with temperature, although less significantly than peak F . Notice that the FWHM of peak F in UTe is increasing with temperature, even as the peak moves toward E_F ,

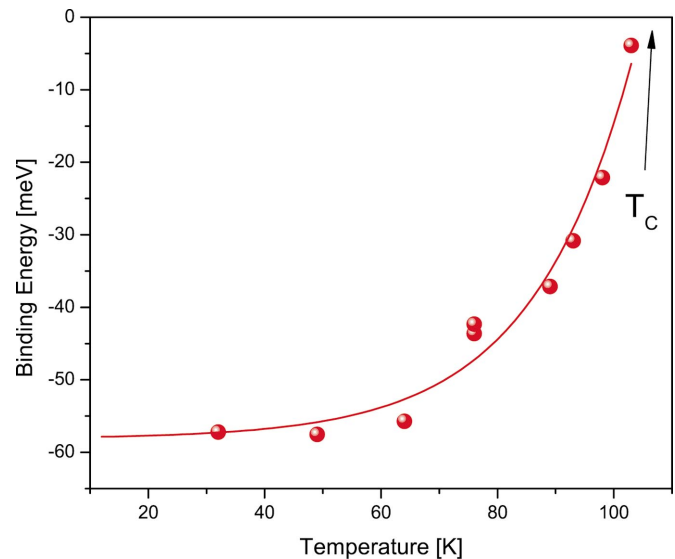


FIG. 10. (Color) Distance of the F peak in UTe from E_F as a function of temperature, showing the band crossing E_F at the ferromagnetic transition.

similar to the photohole lifetime studies in ferromagnetic gadolinium.²⁶

C. NpSb, NpTe

Both NpSb and NpTe order antiferromagnetically at 202 K and 40 K, respectively. Strong mixing of the $5f$ and the p valence states of the anions was deduced from the results of Mössbauer spectroscopy.²⁷ NpTe has the highest γ value 130 mJ/mol/K² amongst all the rocksalt actinide compounds, see Table I or Ref. 28. As far as we know, no photoemission data for these compounds are available in the literature. Our angle-integrated spectra taken at 40.8 eV are shown in Figs. 2 and 3. Similar to the U counterparts, the Sb compound represents a more localized scenario with one relatively broad peak situated around 700 meV below E_F . There seems to be no appreciable F peak in NpSb and only a relatively small feature pinned to E_F in NpTe. A photon-energy dependent study taken with the LPLS at Los Alamos of NpSb, shown in Fig. 12, indicates no significant spectral changes between the signals obtained with incident energies varying from 40.8 to 110 eV, except for broadening due to the instrument resolution gradually worsening in absolute terms as the photon energy is raised. This result suggests a certain amount of hybridization of the $5f$ and conduction-electron states.

D. PuSb, PuTe

PuSb orders antiferromagnetically at 85 K and becomes a ferromagnet at 70 K. Historically, it has been considered to be a typical example of an actinide compound with localized $5f$ electrons. An overriding consideration is the magnetic moment, which is close to the expected value for a $\text{Pu}^{3+}:5f^5$ configuration, and the shape of the magnetic form factor.²⁹ Because of the partial cancellation of the orbital and spin moments in the $5f^5$ configuration with $L=5$, and $S=-5/2$, the momentum dependence of the neutron cross section has a

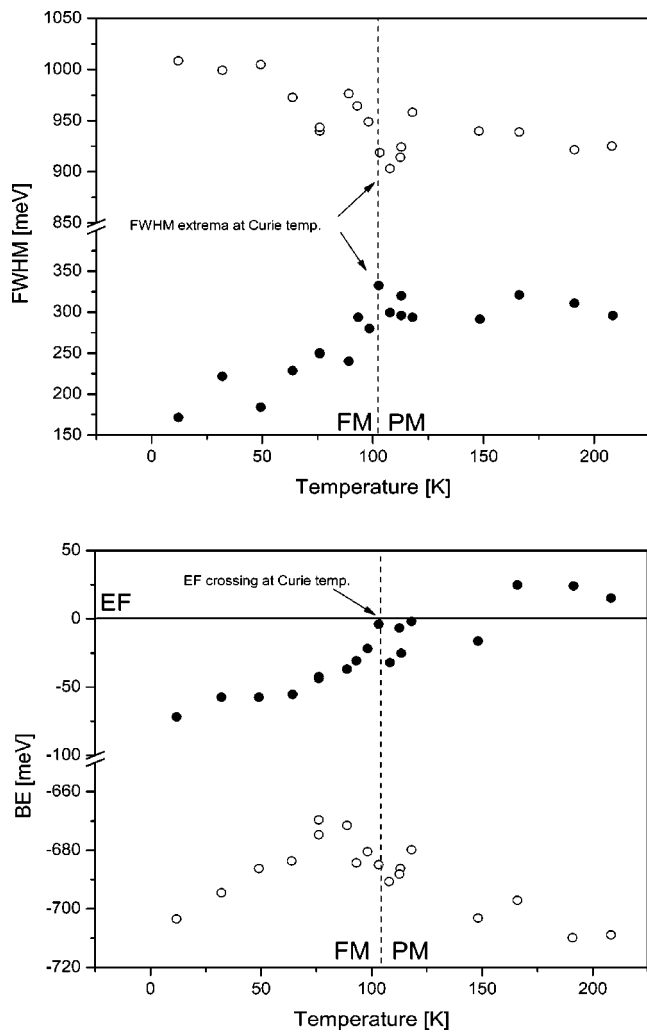


FIG. 11. FWHM and BE of peak *F* (closed points) and peak *B* (open points) for UTe as a function of temperature. FM and PM denote ferromagnetic and paramagnetic states, respectively.

characteristic “hump” so that there is not a maximum at *Q* (the momentum transfer)=0. Since, this effect can *only* arise from such a cancellation it points very strongly to a Pu³⁺ (almost) localized ground state. It should, however, be mentioned that neutron inelastic scattering¹ paints a slightly more complex picture, in which there is certainly room for hybridization between the 5*f* and conduction-electron states.

PuTe exhibits a temperature-independent, but relatively large, susceptibility and a complex electronic structure as seen near *E_F* by photoemission (see Figs. 2 and 3). It might, in fact, have the highest Pauli susceptibility of any material. In PuTe at least four distinct peaks are recognized within the first 2.5 eV from *E_F*. The so-called three-peak manifold, first described in the work on thin films of PuSe³ is also found in PuTe. The nature of the three-peak manifold is still somewhat controversial, but one may clearly notice from the photon energy dependence (Fig. 13) that all three peaks plus peak *B* represent a similar compositional distribution of 5*f* and/or conduction state character, with no dependence on the incident photon energy. This is made clear by plotting the signals from the 40.8 eV light together with the spectra taken

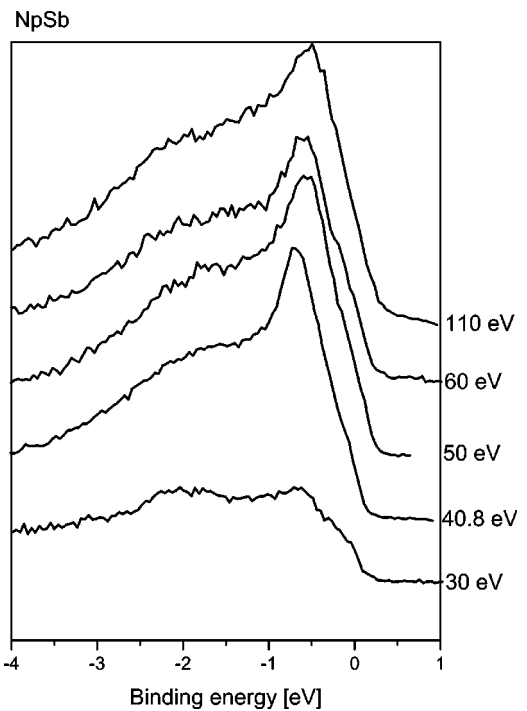


FIG. 12. Photon energy dependent study of NpSb.

at 76 eV, and making a broadening of the former to simulate the resolution of the latter. Figure 14 shows that these spectra overlap completely. Low photon energy scan (at 21.2 eV) in Fig. 13 shows substantial contribution of Te5*p* as well as Pu*d* character superimposed on the secondary electron background.

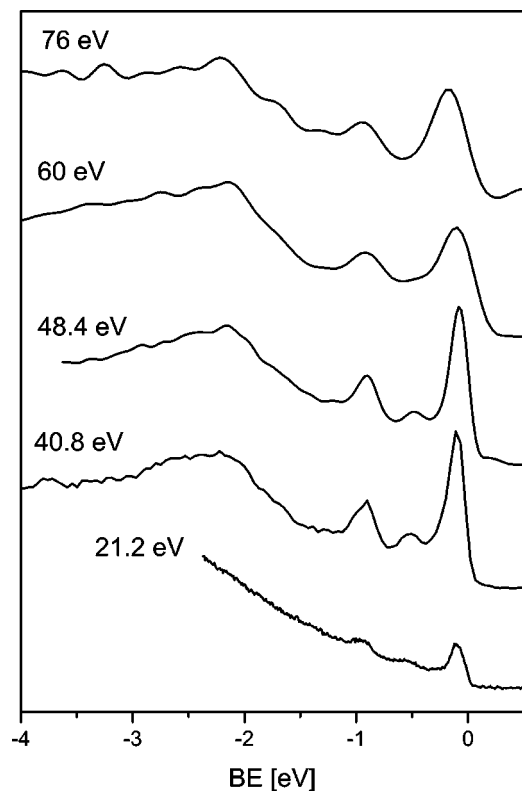


FIG. 13. PuTe photon energy dependent study.

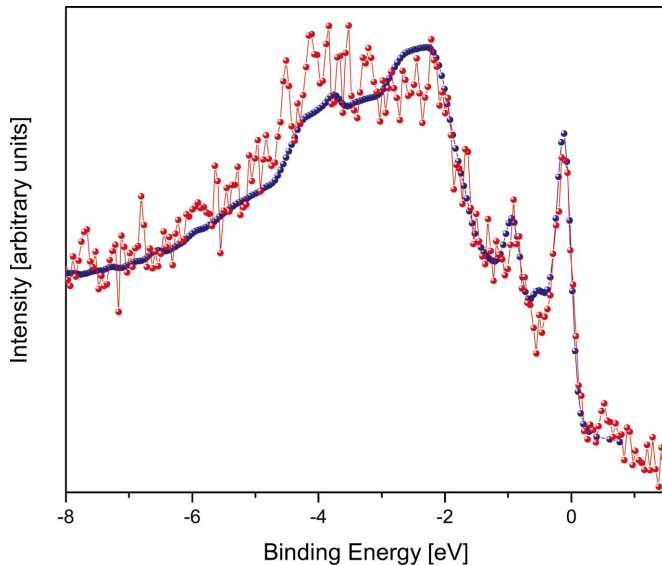


FIG. 14. (Color) PuTe. The 40.8 eV scan (blue line + points) is Gaussian-broadened here to simulate the 76 eV resolution from LPLS (raw data red line + points).

The spectra for PuTe presented here and those measured on thin films of PuSe³ are essentially identical. Since the physical properties of PuSe and PuTe are also identical, this is perhaps not surprising, but the question posed before this investigation was whether the three-peak spectra arose from some surface state present in the thin film. We can now argue that this is not the case. The films have an indeterminate crystallinity, whereas the single crystal surfaces have been laser ablated in the present studies. The fact that the spectra from these differently prepared materials are identical strongly suggests that the spectra are intrinsic to the material and represent the true electronic structure. Interestingly, the same type of spectral features are found in δ -Pu³⁰ and a series of compounds in the Pu-Si system,³¹ but not with the same intensity as in the Pu chalcogenides.

The broadest features, *B*, in the PuTe and in PuSb spectra are assumed to represent the localized *5f* multiplet of unresolved nature. PuSb is indeed the most localized case among all those discussed here, having almost no *5f* spectral weight at E_F .

IV. CONCLUSIONS

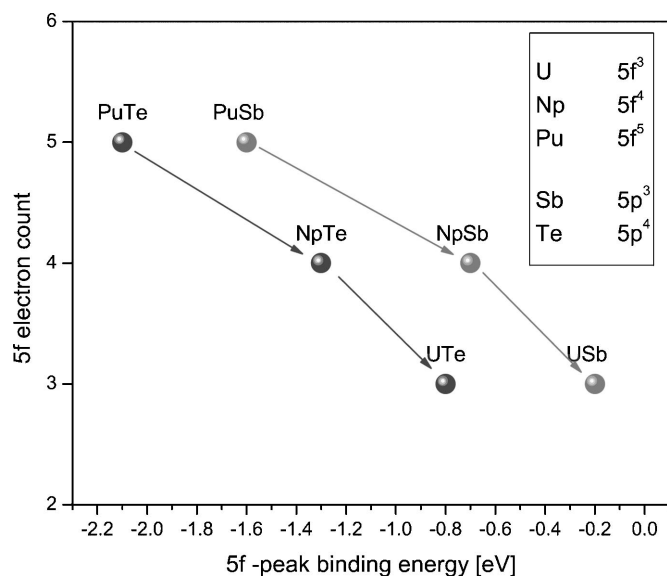
The first, perhaps surprising, point is that in most cases there is *no* or *weak* dependence of the photoemission spectra of these compounds on the incident photon energy. This implies that *in all cases* we are observing features that are predominantly *5f* in character. Even in the case of USb, being the most hybridized of all the compounds investigated here, the dominant *5f* character is found in the spectra (see Fig. 6). Of course, if the amount of *6d*-*7s* admixture changes by $\pm 20\%$ in the different compounds we do not have the sensitivity to observe this, but it can be completely excluded that part of the spectra comes from the *5f* states, and another part from the conduction states. This is somewhat in contradiction with the conclusions of Reihl *et al.*,²⁰ but we argue that

the resolution in that study of 100 meV was insufficient and it is quite probable that in varying the energy the changing resolution in both energy *and* momentum space led to incorrect conclusions.

The second major point we bring to the study of these materials is the *k*-dependent response in USb and UTe, as shown in Figs. 4, 5, and 8. Our high resolution ARPES data show at least two surprises. The first, in USb, is that despite strong indications that this material is a rather localized system, there is a strong *k* dependence of the valence band spectral weight. It might be worth noting that in USb₂ we have previously observed a similar but smaller, 14 meV dispersion of the peak being found around 45 meV below E_F .³² This holds for both the smaller response, presumably from the quasiparticles that come from hybridized *5f*-conduction band states, as well as the more dominant (peak *B*) response at higher binding energy. Dispersions are clearly seen around the *X* point. Thus, although we disagree with the data interpretation of Kumigashira *et al.*,¹⁴ we do agree with their conclusions that the *5f* states in USb exhibit “dual” character. The second feature of the ARPES that is particularly interesting is the temperature dependence of the quasiparticle response (peak *F*, near E_F) in UTe, as shown in Figs. 9 and 10. This shows a strong and direct connection, despite the fact that our spectra are not spin-dependent, so that the concept of a simple molecular field driving the order can be taken as a first approximation and as the pseudo-gap closes there is then no difference between the spin-up and spin-down population of the states.

In our study ARPES data have *not* been obtained for the transuranium samples. This is most unfortunate given the interesting effects observed in USb and UTe, and it gives strong motivation to try and establish at least *one* beamline in the world where these measurements might be carried out. The difficulty, of course, is that with low-energy photons no windows can be used, so the vacuum at the sample is the same (essentially) as in the synchrotron ring. Contamination by an alpha-emitter thus represents a major safety hazard, and it is understandable that synchrotron operators are reluctant to take this risk. However, methods involving fast valves can and should be developed.

The three-peak structure observed in the Pu chalcogenides appears to be a common feature, and does *not* depend on the nature of the sample preparation. Gouder³³ has argued that this feature arises from the *5f*⁶ intermultiplet transition, transitions from *5f*⁶-*5f*⁵, whereas the peak *B* at higher binding energy represents the stable Pu³⁺ configuration with transition from *5f*⁴-*5f*⁴. The latter represents a “localized” level and should be responsible for the magnetic properties. The intermediate valence nature of the ground state usually precludes an ordered magnetic moment, and we suggest this may be the case here. Wachter *et al.*³⁴⁻³⁶ have argued that the Pu chalcogenides are intermediate valent, and has shown that, as also found in UTe, the Poisson ratio of PuTe is negative. In Ref. 36 the peak at around 4 eV binding energy in PuSe, not well resolved at 40.8 eV photon energy, was proposed to indicate the Pu³⁺ configuration, which is in contrast with earlier attributions.³³ However, from the He_I scans this particular peak in PuSe seems much more like Se4*p* emission, with the peak intensity growing significantly with de-

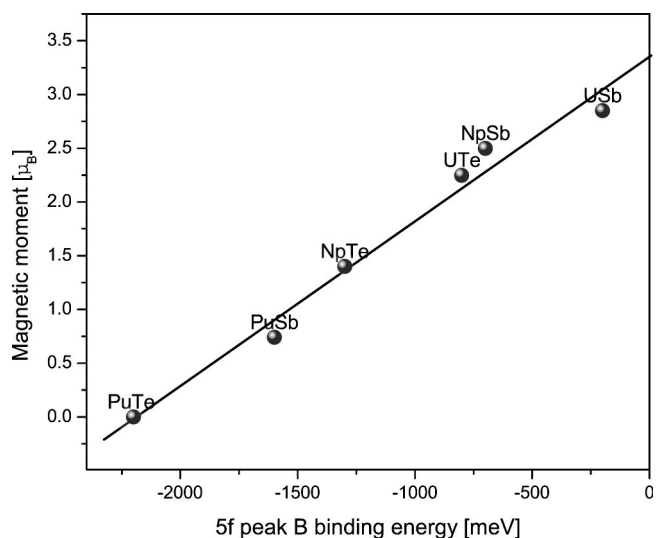
FIG. 15. Systematics in the $5f$ main peak binding energy.

creasing photon energy as expected from the cross-section arguments. In the case of PuTe, this argument indicates that peak B is more likely to represent the Pu^{3+} configuration. An additional problem with the localized multiplet argument for PuTe and PuSe is the position of peak F at the Fermi level. It seems difficult to construct a localized multiplet that forms a part of the Fermi surface. Finally, one could argue also that the intermultiplet nature of the three-peak structure is due to a “surface state” as has been found in a number of Sm compounds,^{37,38} but this is harder to sustain as one would then expect the bulk to be magnetic, and such a surface state should exist also in PuSb, which is clearly not the case.

That the Pu chalcogenides are complex can be judged from the considerable theoretical effort recently devoted to them,^{39,40} but, despite this effort, the absence of magnetism in the chalcogenides, and the high value of the susceptibility, cannot be easily reproduced. From our experiments it would appear that a mixed valence state, in agreement with Wachter *et al.*,^{34–36} is a reasonable basis to start considerations of the Pu-chalcogenides.

Finally, we come to perhaps the most intriguing part of our study. We have argued that the maximum spectral weight is in peak B , as shown in Figs. 1 and 2. We may then ask whether we can extract any systematics from the positions of these peaks and other properties of the system. First we show in Fig. 15 a plot of $5f$ electron count (assuming that all the compounds are trivalent) versus the position of peak B . Peak F can be traced only in a systematic way in the chalcogenide compounds and in this series shows a trend similar to peak B . Addition of one electron, either $\text{An}5f$ or ligand p , shifts the spectral features toward higher binding energies. Within the whole series one can state that Sb counterpart is more localized than the Te compound for each pnictides-chalcogenide pair.

Furthermore, we now plot the ordered magnetic moment at low temperature (Table I) as a function of the binding energy of peak B and the result is shown in Fig. 16. This is a startling relationship. We know that the moments are made

FIG. 16. Magnetic moment systematics within the series as revealed by plotting the ordered magnetic moment of the compound against the binding energy of peak B as observed in photoemission experiments.

up in these compounds from a large (positive) orbital moment and an oppositely directed (negative) spin moment. This cancellation results, for example, in an extrinsically smaller moment for Pu systems, *whatever* the position of peak B . Assuming the J quantum number still applies, $J = 9/2, 4,$ and $5/2$ for $\text{U}^{3+}, \text{Np}^{3+},$ and Pu^{3+} , respectively, and using the intermediate coupling g values, we may calculate the maximum ordered moments as $3.42 \mu_B, 2.57 \mu_B,$ and $1.04 \mu_B$, respectively. In fact no Pu systems are known to have a moment larger than $0.75 \mu_B$. Does this imply (from the figure) that the peak B should always be at least 1.5 eV away from E_F for Pu systems? Another way to realize this is that the Pu compounds are, in general, *more* localized than either U or Np compounds so the peak B may well be pushed further below E_F . On the other hand, the correlation for the U and Np compounds, as well as the relatively similar values of the potential total ordered moments as deduced above, does suggest that a rather simple pseudo-rigid band model might apply. Suppose, for example, that the polarization of the spin-up and spin-down bands is governed by their interaction with the quasiparticle band near E_F , which is already suggested by the temperature dependence found in UTe, Fig. 10. In this case it can be readily seen that the further peak B is displaced from E_F , the smaller will be the polarization and the resulting ordered magnetic moment. To our knowledge such a relationship has never been observed previously in *any* system in the periodic table, and we hope these measurements provide a stimulus for further theoretical work.

ACKNOWLEDGMENTS

This work was supported by the US Department of Energy, Office of Science, Division of Materials Science and Engineering, the LANL-LDRD program and under contract W-7405-ENG-82. This work is also based in part upon re-

search conducted at the Synchrotron Radiation Center, University of Wisconsin-Madison, which is supported by the NSF under Award No. DMR-0084402. G.H.L. would like to thank Los Alamos National Laboratory for the award of a John Wheatley Scholarship, during which time most of this work was completed. The high-purity Np metal used in the

fabrication of single crystals used in this work was made available through a loan agreement between Lawrence Livermore National Laboratory and ITU, in the frame of a collaboration involving LLNL, Los Alamos National Laboratory, and the US Department of Energy. Thanks are due to Ladia Havela and Peter Oppeneer for numerous discussions.

-
- ¹See *Handbook on the Physics and Chemistry of Rare Earths*, edited by K. A. Gschneidner, L. Eyring, G. H. Lander, and G. R. Choppin (Elsevier, Amsterdam, 1993), Vol. 17; Vol. 19 (1994) for a background to the many studies performed on these materials.
- ²G. H. Lander and P. Burllet, *Physica B* **215**, 7 (1995).
- ³T. Gouder, F. Wastin, J. Rebizant, and L. Havela, *Phys. Rev. Lett.* **84**, 3378 (2000).
- ⁴J. C. Spirlet and O. Vogt, in *Handbook on the Physics and Chemistry of the Actinides*, edited by A. J. Freeman and G. H. Lander, (Elsevier, Amsterdam, 1984), Vol. 1, p. 79.
- ⁵T. Durakiewicz, Al Arko, J. J. Joyce, D. P. Moore, and K. Graham, *Rev. Sci. Instrum.* **73**, 3750 (2002).
- ⁶A. J. Arko, J. J. Joyce, and L. Morales, *J. Alloys Compd.* **286**, 14 (1999).
- ⁷J. J. Joyce, A. J. Arko, L. E. Cox, and S. Czuchlewski, *Surf. Interface Anal.* **26**, 121 (1998).
- ⁸B. Reihl, N. Martensson, and O. Vogt, *J. Appl. Phys.* **53**, 2008 (1982).
- ⁹G. H. Lander and W. G. Stirling, *Phys. Rev. B* **21**, 436 (1980); B. Halg and A. Furrer, *ibid.* **34**, 6258 (1986).
- ¹⁰H. Rudigier, H. R. Ott, and O. Vogt, *Phys. Rev. B* **32**, 4584 (1985).
- ¹¹A. Ochiai, E. Hotta, Y. Haga, T. Suzuki, Y. Suzuki, T. Shikama, and K. Suzuki, *Physica B* **206-207**, 789 (1995).
- ¹²A. Ishiguro, H. Aoki, O. Sugie, M. Suzuki, A. Sawada, N. Sato, T. Komatsubara, A. Ochiai, T. Suzuki, K. Suzuki, M. Higuchi, and A. Hasegawa, *J. Appl. Phys.* **66**, 2764 (1997).
- ¹³K. Knöpfle and L. M. Sandratskii, *Phys. Rev. B* **63**, 014411 (2000).
- ¹⁴H. Kumigashira, T. Ito, A. Ashihara, H. D. Kim, H. Aoki, T. Suzuki, H. Yamgami, and T. Takahashi, *Phys. Rev. B* **61**, 15707 (2000).
- ¹⁵N. Beatham, P. A. Cox, A. F. Orchard, and I. P. Grant, *Chem. Phys. Lett.* **63**, 69 (1979).
- ¹⁶B. Reihl, G. Hollinger, and F. J. Himpsel, *Phys. Rev. B* **28**, 1490 (1983).
- ¹⁷P. Erdos and J. Robinson, *The Physics of Actinide Compounds* (Plenum, New York, 1983).
- ¹⁸H. Bilz, G. Gunterherodot, W. Kleppmann, and W. Kress, *Phys. Rev. Lett.* **43**, 1998 (1979).
- ¹⁹J. Schoenes, B. Frick, and O. Vogt, *Phys. Rev. B* **30**, 6578 (1984).
- ²⁰B. Reihl, N. Martensson, P. Heiman, D. E. Eastman, and O. Vogt, *Phys. Rev. Lett.* **46**, 1480 (1981).
- ²¹G. H. Lander, W. G. Stirling, J. M. Rossat-Mignod, M. Hagen, and O. Vogt, *Phys. Rev. B* **41**, 6899 (1990).
- ²²G. H. Lander, W. G. Stirling, and B. R. Cooper, *Can. J. Phys.* **73**, 718 (1995).
- ²³G. J. Hu and B. R. Cooper, *Phys. Rev. B* **48**, 12743 (1993).
- ²⁴T. Shishidou and T. Oguchi, *Phys. Rev. B* **62**, 11747 (2000).
- ²⁵P. R. Norton, R. L. Tapping, D. K. Creber, and W. J. L. Buyers, *Phys. Rev. B* **21**, 2572 (1980).
- ²⁶A. V. Fedorov, T. Valla, F. Liu, P. D. Johnson, M. Weinert, and P. B. Allen, *Phys. Rev. B* **65**, 212409 (2002).
- ²⁷J. P. Sanchez, P. Burllet, S. Quezel, D. Bonnissseau, and J. Rossat-Mignod, *Solid State Commun.* **67**, 999 (1988).
- ²⁸G. R. Steward, R. G. Haire, J. C. Spirlet, and J. Rebizant, *J. Alloys Compd.* **177**, 167 (1991).
- ²⁹G. H. Lander, A. Delaplame, P. J. Brown, J. C. Spirlet, J. Rebizant, and O. Vogt, *Phys. Rev. Lett.* **53**, 2262 (1984).
- ³⁰L. Havela, T. Gouder, F. Wastin, and J. Rebizant, *Phys. Rev. B* **65**, 235118 (2002).
- ³¹T. Gouder, F. Wastin, P. Boulet, E. Colineau, J. Rebizant, and F. Huber (unpublished).
- ³²E. Guziewicz, T. Durakiewicz, M. T. Butterfield, C. G. Olson, J. J. Joyce, A. J. Arko, J. L. Sarrao, D. P. Moore, and L. Morales, *Phys. Rev. B* **69**, 045102 (2004).
- ³³T. Gouder, *J. Electron Spectrosc. Relat. Phenom.* **101**, 419 (1999).
- ³⁴P. Wachter, F. Marabelli, and B. Bucher, *Phys. Rev. B* **43**, 11136 (1991).
- ³⁵P. Wachter, M. Filzmoser, and J. Rebizant, *Physica B* **293**, 199 (2001).
- ³⁶P. Wachter, *Solid State Commun.* **127**, 599 (2003).
- ³⁷A. Stenborg, O. Bjorneholm, A. Nilsson, N. Mårtensson, J. N. Andersen, and C. Wigren, *Phys. Rev. B* **40**, 5916 (1989).
- ³⁸F. Strisland, S. Raaen, A. Ramsted, and C. Berg, *Phys. Rev. B* **55**, 1391 (1997).
- ³⁹P. M. Oppeneer, T. Kraft, and M. S. S. Brooks, *Phys. Rev. B* **61**, 12825 (2000).
- ⁴⁰L. Petit, A. Svane, W. M. Temmerman, and S. Szotek, *Eur. Phys. J. B* **25**, 139 (2002).
- ⁴¹R. O. A. Hall, A. J. Jeffery, M. Mortimer, and J. C. Spirlet, *J. Less-Common Met.* **121**, 181 (1986).